

SIMULATING COULOMB AND LOG-GASES WITH HYBRID MONTE CARLO ALGORITHMS

DJALIL CHAFAÏ AND GRÉGOIRE FERRÉ

ABSTRACT. Coulomb and log-gases are exchangeable singular Boltzmann–Gibbs measures appearing in mathematical physics at many places, in particular in random matrix theory. We explore experimentally an efficient numerical method for simulating such gases. It is an instance of the Hybrid or Hamiltonian Monte Carlo algorithm, in other words a Metropolis–Hastings algorithm with proposals produced by a kinetic or underdamped Langevin dynamics. This algorithm has excellent numerical behavior despite the singular interaction, in particular when the number of particles gets large. It is more efficient than the well known overdamped version previously used for such problems.

CONTENTS

1. Boltzmann–Gibbs measures	2
1.1. Coulomb gases	2
1.2. Log-gases	3
1.3. Static energy and equilibrium measures	3
1.4. Two remarkable gases from random matrix theory	4
2. Simulating log-gases and Coulomb gases	5
2.1. Standard sampling methods	6
2.2. Hybrid Monte Carlo algorithm	7
3. Numerical experiments on remarkable models	10
3.1. Case study: 1D	10
3.2. Case study: 2D	10
3.3. Case study: 3D	10
Appendix A. Julia code	10
Acknowledgments	14
References	14

We explore the numerical simulation of Coulomb gases and log-gases by mean of Hybrid or Hamiltonian Monte Carlo algorithms (HMC). Such algorithms consist basically in using discretized kinetic or underdamped Langevin dynamics to produce proposals for Metropolis–Hastings algorithms. This can be viewed as a way to add momentum to a Monte Carlo interacting particle system. The basic outcome of this exploratory work is that HMC algorithms have remarkably good numerical behavior for such gases despite the singularity of the interactions. Such algorithms scale well with the dimension of the system, see [4, 8]. They are therefore more efficient than the tamed overdamped version already explored in the literature for instance in [44]. In this paper, we benchmark the capability of the algorithm to reproduce known results efficiently, and we make it ready to explore new conjectures.

Date: Spring 2018, compiled August 3, 2022.

2000 Mathematics Subject Classification. 65C05 (Primary); 82C22; 60G57.

Key words and phrases. Numerical Simulation; Random number generator; Singular Stochastic Differential Equation; Coulomb gas; Monte Carlo Adjusted Langevin; Hybrid Monte Carlo; Markov Chain Monte Carlo; Langevin dynamics; Kinetic equation.

Another advantage of this approach is that it could be adapted to take into account a sub-manifold constraint [42]. For instance, this could be used for simulating random matrices with prescribed trace or determinant, which is difficult to achieve by direct sampling of matrices.

1. BOLTZMANN–GIBBS MEASURES

We are interested in interacting particle systems subject to an external field and experiencing singular pair interactions. In order to encompass Coulomb gases as well as log-gases from random theory, we introduce a vector subspace S of dimension d of \mathbb{R}^n , with $n \geq 2$ and $n \geq d \geq 1$. The particles belong to S , and \mathbb{R}^n is understood as a physical ambient space. We equip S with the trace of the Lebesgue measure of \mathbb{R}^n , denoted by dx . The external field and the pair interaction are respectively denoted by $V : S \mapsto \mathbb{R}$ and $W : S \mapsto (-\infty, +\infty]$, and belong to \mathcal{C}^2 functions, with $W(x) < \infty$ for all $x \neq 0$. For any $N \geq 2$, we consider the probability measure P_N on $S^N = S \times \cdots \times S$ defined by

$$P_N(dx) = \frac{e^{-\beta_N H_N(x_1, \dots, x_N)}}{Z_N} dx_1 \cdots dx_N, \quad (1.1)$$

where $\beta_N > 0$ is a parameter,

$$Z_N = \int_{S^N} e^{-\beta_N H_N(x_1, \dots, x_N)} dx_1 \cdots dx_N$$

is the normalizing factor, and

$$H_N(x_1, \dots, x_N) = \frac{1}{N} \sum_{i=1}^N V(x_i) + \frac{1}{2N^2} \sum_{i \neq j} W(x_i - x_j)$$

is usually called energy or Hamiltonian of the system. We assume that β_N , V , and W are chosen in such a way that $Z_N < \infty$ for any N . The law P_N is invariant by permutation of the coordinates x_1, \dots, x_N (exchangeable), and H_N depends only on the empirical measure

$$\mu_N = \frac{1}{N} \sum_{i=1}^N \delta_{x_i}.$$

Therefore P_N is also the law of a random empirical measure encoding a cloud of indistinguishable particles x_1, \dots, x_N . We emphasize that the particles live on the space $S^N = S \times \cdots \times S$ of dimension dN . The parameter n serves as the physical dimension of the ambient space, for the Coulomb gas setting described next.

For any $n \geq 1$ and $x \in \mathbb{R}^n$, we denote by $|x| = \sqrt{x_1^2 + \cdots + x_n^2}$ the Euclidean norm of x . This matches the absolute value when $n = 1$ and the modulus when $n = 2$ with $\mathbb{R}^2 \equiv \mathbb{C}$.

1.1. Coulomb gases. The notion of Coulomb gas is based on elementary electrostatics. Here the vector subspace S is interpreted as a conductor. It corresponds to take $W = g$ where g is the Coulomb kernel or Green function in the physical space \mathbb{R}^n . More precisely, recall that the Green function g in \mathbb{R}^n , $n \geq 2$, is defined for all $x \in \mathbb{R}^n$, $x \neq 0$, by

$$g(x) = \begin{cases} \log \frac{1}{|x|} & \text{if } n = 2, \\ \frac{1}{|x|^{n-2}} & \text{if } n \geq 3. \end{cases}$$

This function is the fundamental solution of the Poisson equation, namely, denoting Δ the Laplace operator in \mathbb{R}^n and δ_0 the Dirac mass at 0, we have, in the sense of distributions,

$$-\Delta g = c\delta_0, \quad \text{with } c = \begin{cases} 2\pi & \text{if } n = 2, \\ (n-2)|\mathbb{S}^{n-1}| = \frac{n(n-2)\pi^{n/2}}{\Gamma(1+n/2)} & \text{if } n \geq 3. \end{cases}$$

The physical interpretation in terms of electrostatics is as follows: $H_N(x_1, \dots, x_N)$ is the electrostatic energy of a configuration of N electrons in \mathbb{R}^n lying on S at positions x_1, \dots, x_N , in an external field given by the potential V . The Green function or Coulomb kernel g expresses the Coulomb repulsion which is a two body singular interaction. The probability measure P_N can be seen as a Boltzmann–Gibbs measure, β_N playing the role of an inverse temperature. The probability measure P_N is known as a Coulomb gas or as a one-component plasma, see for instance [53] and references therein.

1.2. Log-gases. A log-gas corresponds to choosing $d = n$ and a logarithmic interaction W whatever the value of n is, namely

$$W(x) = \log \frac{1}{|x|} = -\frac{1}{2} \log(x_1^2 + \dots + x_d^2), \quad x \in S.$$

Coulomb gases and log-gases coincide when $d = n = 2$. In dimension $d = n \geq 3$, log-gases are natural and classical objects of approximation theory and can be seen as limiting Riesz potentials namely $\lim_{\alpha \rightarrow 0} \frac{1}{\alpha} (|x|^{-\alpha} - 1)$, see for instance [55, 54, 53].

1.3. Static energy and equilibrium measures. Under natural assumptions over V and W , typically when $\beta_N \gg N$ and V beats W at infinity, it is well known, see for instance [11, 52] and references therein, that P_N almost surely, the empirical measure

$$\mu_N = \frac{1}{N} \sum_{i=1}^N \delta_{x_i}$$

tends as $N \rightarrow \infty$ to a non random probability measure, the equilibrium measure

$$\mu_* = \arg \inf \mathcal{E},$$

the unique minimizer of the strictly convex lower semi-continuous “energy” \mathcal{E} defined by

$$\mu \mapsto \mathcal{E}(\mu) = \int V d\mu + \iint W(x-y) \mu(dx) \mu(dy).$$

When $W = g$ is the Coulomb kernel, the quantity $\mathcal{E}(\mu)$ is the electrostatic energy of the distribution of charges μ , formed by the sum of the electrostatic potential coming from the external electric field V with the Coulomb self repulsion by mean of the Coulomb kernel g . Note that $\mathcal{E}(\mu) = \infty$ if μ has a Dirac mass due to the singularity of g . An Euler–Lagrange variational analysis reveals that when $S = \mathbb{R}^d$ and V is smooth, convex, and grows faster than g at infinity then the equilibrium probability measure μ_* is compactly supported and has density proportional to ΔV , see [11] and references therein. Figure 1 gives examples of equilibrium measures in this Coulomb setting. We refer to [35, 29, 50, 52, 53] for old and new potential theory from this analytic point of view. Quite a few equilibrium measures are known for log-gases beyond Coulomb gases, see for instance [13].

d	S	n	V	μ_*	Nickname
1	\mathbb{R}	2	$\infty \mathbf{1}_{\text{interval}^c}$	arcsine	
1	\mathbb{R}	2	x^2	semicircle	GUE
2	\mathbb{R}^2	2	$ x ^2$	uniform on a disc	Ginibre
$d \geq 3$	\mathbb{R}^d	d	$ x ^2$	uniform on a ball	
$d \geq 3$	\mathbb{R}^d	d	radial	radial in a ring	

FIGURE 1. Examples of equilibrium measures for Coulomb gases, see [50, 11].

Actually it can be shown that essentially if $\beta_N \gg N$ and V beats g at infinity then under $(P_N)_N$ the sequence of random empirical measures $(\mu_N)_N$ satisfies a large deviation principle with speed β_N and good rate function \mathcal{E} , see [11, 27, 3]. Concentration of measure inequalities are also available, see [14] and references therein.

1.4. Two remarkable gases from random matrix theory. Let us give a couple of famous gases from random matrix theory that will serve as benchmark for our algorithm. They correspond to $n = 2$ because the Lebesgue measure on a matrix translates via the Jacobian of the change of variable as a Vandermonde determinant on the eigenvalues, giving rise to the two-dimensional Coulomb kernel inside the exponential via the identity

$$\prod_{i < j} |x_i - x_j| = \exp\left(\sum_{i < j} \log |x_i - x_j|\right).$$

Hence the name “log-gases”. A good reference on this subject is [25] and we refer to [22, 19, 25, 26, 33] for more examples of Coulomb gases related to random matrix models. Coulomb gases remain interesting in any dimension n beyond random matrices, see [52, 53].

Beta-Hermite model. This model corresponds to

$$d = 1, n = 2, S = \mathbb{R}, V(x) = \frac{x^2}{2\beta}, W(x) = -\log |\cdot|, \beta_N = N^2\beta, \beta \in (0, \infty).$$

This means that the particles evolve on the line \mathbb{R} with Coulomb interactions given by the Coulomb kernel in \mathbb{R}^2 . For $\beta = 2$, it becomes the famous Gaussian Unitary Ensemble (GUE), which is the distribution of the eigenvalues of random $N \times N$ Hermitian matrices distributed according to the Gaussian probability measure with density proportional to $H \mapsto e^{-N\text{Tr}(H^2)}$. Beyond the case $\beta = 2$, the cases $\beta = 1$ and $\beta = 4$ correspond respectively to Gaussian random matrices with real and quaternionic entries. Following [19], for all $\beta \in (0, \infty)$, the measure P_N is also the distribution of the eigenvalues of special random $N \times N$ Hermitian tridiagonal matrices with independent but non identically distributed entries. Back to the case $\beta = 2$, the law P_N writes

$$(x_1, \dots, x_N) \in \mathbb{R}^N \mapsto e^{-\frac{N}{2} \sum_{i=1}^N x_i^2} \prod_{i < j} (x_i - x_j)^2. \quad (1.2)$$

In this case, the Coulomb gas P_N has a determinantal structure, making it integrable or exactly solvable for any $N \geq 2$, see [45, 25]. This provides in particular a formula for the density of the mean empirical spectral distribution $\mathbb{E}\mu_N$ under P_N , namely

$$x \in \mathbb{R} \mapsto \frac{e^{-\frac{N}{2}x^2}}{\sqrt{2\pi N}} \sum_{\ell=0}^{N-1} H_\ell^2(\sqrt{N}x), \quad (1.3)$$

where $(H_\ell)_{\ell \geq 0}$ are the Hermite polynomials which are the orthonormal polynomials for the standard Gaussian distribution $\mathcal{N}(0, 1)$. The equilibrium measure μ_* in this case is the Wigner semicircle distribution with the following density with respect to the Lebesgue measure:

$$x \in \mathbb{R} \mapsto \frac{\sqrt{4 - x^2}}{2\pi} \mathbf{1}_{x \in [-2, 2]}. \quad (1.4)$$

A plot of μ_* and $\mathbb{E}\mu_N$ is provided in, Figure 2, together with our simulations. We refer to [37] for a direct proof of convergence of (1.3) to (1.4) as $N \rightarrow \infty$. Beyond the case $\beta = 2$, the equilibrium measure μ_* is still a Wigner semicircle distribution, scaled by β , supported by the interval $[-\beta, \beta]$, but up to our knowledge we do not have a formula for the mean empirical spectral distribution $\mathbb{E}\mu_N$, except when β is an even integer, see [19].

Beta-Ginibre model. This model corresponds to

$$d = 2, n = 2, S = \mathbb{R}^2, V(x) = \frac{|x|^2}{\beta}, W(x) = -\log |x|, \beta_N = N^2\beta, \beta \in (0, \infty).$$

In this case, the particles move in \mathbb{R}^2 with a Coulomb repulsion of dimension 2 – it is therefore a Coulomb gas. As for the GUE, the law P_N can be written as

$$(x_1, \dots, x_N) \in (\mathbb{R}^2)^N \mapsto e^{-N \sum_{i=1}^N |x_i|^2} \prod_{i < j} |x_i - x_j|^\beta, \quad (1.5)$$

When $\beta = m$ for an even integer $m \in \{2, 4, \dots\}$, the distribution of this gas matches the Laughlin wavefunction modeling the fractional quantum Hall effect (FQHE), see for instance [24].

For $\beta = 2$, this gas, known as the complex Ginibre Ensemble, matches the distribution of the eigenvalues of random $N \times N$ complex matrices distributed according to the Gaussian probability measure with density proportional to $M \mapsto e^{-N\text{Tr}(MM^*)}$ where $M^* = \overline{M}^\top$. In this case P_N has a determinantal structure, see [45, 25]. This provides a formula for the density of the mean empirical spectral distribution $\mathbb{E}\mu_N$ under P_N , namely

$$x \in \mathbb{R}^2 \mapsto \frac{e^{-N|x|^2}}{\pi} \sum_{\ell=0}^{N-1} \frac{|\sqrt{N}x|^{2\ell}}{\ell!}, \quad (1.6)$$

which is the analogue of (1.3) for the Gaussian Unitary Ensemble. If Y_1, \dots, Y_N are independent and identically distributed Poisson random variables of mean $|x|^2$ for some $x \in \mathbb{R}^2$ then (1.6) writes

$$x \in \mathbb{R}^2 \mapsto \frac{1}{\pi} \mathbb{P}\left(\frac{Y_1 + \dots + Y_N}{N} < 1\right).$$

As $N \rightarrow \infty$, by the law of large numbers, it converges to $1/\pi$ if $|x| < 1$ and to 0 if $|x| > 1$, while by the central limit theorem it converges to $1/(2\pi)$ if $|x| = 1$. It follows that $\mathbb{E}\mu_N$ converges weakly as $N \rightarrow \infty$ to the uniform distribution on the disk, with density

$$x \in \mathbb{R}^2 \mapsto \frac{\mathbf{1}_{|x|<1}}{\pi}, \quad (1.7)$$

which is the equilibrium measure μ_* . When N is finite, the numerical evaluation of (1.6) is better done by mean of the Gamma law. Namely, by induction and integration by parts, (1.6) writes

$$x \in \mathbb{R}^2 \mapsto \frac{1}{\pi(N-1)!} \int_{N|x|^2}^{\infty} u^{N-1} e^{-u} du = \frac{\Gamma(N, N|x|^2)}{\pi},$$

where Γ is the normalized incomplete Gamma function and where we used the identity

$$e^{-r} \sum_{\ell=0}^{N-1} \frac{r^\ell}{\ell!} = \frac{1}{(N-1)!} \int_r^{\infty} u^{N-1} e^{-u} du.$$

Note that $t \mapsto 1 - \Gamma(N, t)$ is the cumulative distribution function of the Gamma distribution with shape parameter N and scale parameter 1. Figure 4 illustrates the difference between the limiting distribution (1.7) and the mean empirical spectral distribution (1.6) for a finite N . Beyond the case $\beta = 2$, we no longer have a formula for the density of $\mathbb{E}\mu_N$, but a simple scaling argument reveals that the equilibrium measure μ_* is in this case the uniform distribution on the centered disk of radius $\sqrt{\beta/2}$.

2. SIMULATING LOG-GASES AND COULOMB GASES

Regarding simulation of log-gases or Coulomb gases such as (1.1), it is natural to use the random matrix models when they are available. There exist also methods specific to determinantal processes which cover the log-gases of random matrix theory with $\beta = 2$, see [31, 51, 47, 16, 2, 36, 28]. Beyond these specially structured cases, a great variety of methods are available for simulating Boltzmann–Gibbs measures, such as overdamped Langevin diffusion algorithm, Metropolis–Hastings algorithm, Metropolis adjusted Langevin algorithm (MALA), and kinetic versions called Hybrid or Hamiltonian Monte Carlo (HMC) which are based on a kinetic (or underdamped) Langevin diffusion, see for instance [9, 43, 21].

Two difficulties arise when sampling measures as (1.1). First, the Hamiltonian H_N involves all couples, so the computation of forces and energy scales quadratically with

the number of particles. A natural way to circumvent this numerical problem is to use clusterization procedures such as the “fast multipole methods”, see for instance [30]. A second difficult feature of such a Hamiltonian is the singularity of the interacting function W , which typically results in numerical instability. A standard stabilization procedure is to «tame» the dynamics [32, 10], which is the strategy adopted in [44]. However, this smoothing of the force induces a supplementary bias in the invariant measure, as shown in [10] for regular Hamiltonians H_N . This leads to using small time steps, hence long computations. In the present note, we explore for the first time the usage of HMC for general Coulomb gases in the context of random matrices, in the spirit of [57], the difficulty being the singularity of the interaction. This method has the advantage of sampling the exact invariant measure (1.1), while allowing to choose large time steps, which reduces the overall computational cost.

In Section 2.1, we review standard methods for sampling measure of the form $e^{-\beta_N H_N}$, before presenting in detail the HMC algorithm in Section 2.2.

2.1. Standard sampling methods. To simplify and from now on, we suppose the support set S in (1.1) to be \mathbb{R}^d . We introduce the methods based on the overdamped Langevin dynamics. To sample approximately (1.1), the idea is to exploit the fact that P_N in (1.1) is the reversible invariant probability measure of the Markov diffusion process $(X_t)_{t \geq 0}$ solution to the stochastic differential equation:

$$dX_t = -\alpha_N \nabla H_N(X_t) dt + \sqrt{2 \frac{\alpha_N}{\beta_N}} dB_t, \quad (2.1)$$

or in other words

$$X_t = X_0 - \alpha_N \int_0^t \nabla H_N(X_s) ds + \sqrt{2 \frac{\alpha_N}{\beta_N}} B_t,$$

where $(B_t)_{t \geq 0}$ is a standard Brownian motion on S^N and $\alpha_N > 0$ is an arbitrary time scaling parameter (for instance $\alpha_N = 1$ or $\alpha_N = \beta_N$). The infinitesimal generator associated with (2.1) is

$$Lf = \frac{\alpha_N}{\beta_N} \Delta f - \alpha_N \nabla H_N \cdot \nabla f.$$

The difficulty in solving (2.1) lies in the fact that the energy H_N involves a singular interaction W , which may lead the process to explode. Actually, under certain conditions on β_N and V , the equation (2.1) is well posed, the process $(X_t)_{t \geq 0}$ is well defined, and

$$X_t \xrightarrow[t \rightarrow \infty]{\text{Law}} P_N,$$

for all non-degenerate initial condition X_0 . See for instance [1, 23, 15] for the case of Beta-Hermite case known as the Dyson Ornstein-Uhlenbeck process, and [6] for the Beta-Ginibre case. We do not discuss these delicate aspects in this note. A convergence in Cesàro mean is provided by the ergodic theorem for additive functionals,

$$\frac{1}{t} \int_0^t \delta_{X_s} ds \xrightarrow[t \rightarrow \infty]{\text{weak}} P_N$$

almost surely or, for any test function $f \in L^1(P_N)$,

$$\frac{1}{t} \int_0^t f(X_s) ds \xrightarrow[t \rightarrow \infty]{} \int_S f dP_N.$$

It is also possible to accelerate the convergence by adding a divergence free term in the dynamics (2.1), see for instance [20, 40] and references therein. This modification keeps the same invariant distribution but produces a non-reversible dynamics called sometimes non-equilibrium dynamics.

This method of simulation is referred to as an “unadjusted Langevin algorithm”, a terminology which will be clarified later on. In practice, one cannot simulate the continuous

stochastic process $(X_t)_{t \geq 0}$ solution to (2.1), and resorts to a numerical integration with a finite time step Δt . A typical choice is the Euler–Maruyama scheme [34, 46], which reads

$$x_{k+1} = x_k - \nabla H_N(x_k) \alpha_N \Delta t + \sqrt{2 \frac{\alpha_N}{\beta_N} \Delta t} G_k, \quad (2.2)$$

where (G_k) is a family of independent and identically distributed standard Gaussian variables. Note that α_N and Δt play the same role here. However, because of the singularity of H_N , this sampling scheme leads to important biases in practice. One way to stabilize the dynamics is to use a tamed version of (2.2), which typically takes the following form:

$$x_{k+1} = x_k - \frac{\nabla H_N(x_k) \alpha_N \Delta t}{1 + |\nabla H_N(x_k)| \alpha_N \Delta t} + \sqrt{2 \frac{\alpha_N}{\beta_N} \Delta t} G_k. \quad (2.3)$$

This strategy is used in [44] but, as noted by the authors, the time step needed to reach convergence scales as $\Delta t \sim N^{-2}$, which makes the study of large systems difficult.

Another strategy is to add a selection step at each iteration. This is the idea of the Metropolis Adjusted (overdamped) Langevin Algorithm (MALA), which prevents irrelevant moves with a Metropolis step. One can also view the MALA algorithm as a Metropolis algorithm in which the proposal is produced by using a one step discretization of the Langevin dynamics (2.1). Let us make this precise; more details can be found *e.g.* in [48].

Algorithm 2.1 (Metropolis Adjusted (overdamped) Langevin Algorithm – MALA). *Let K be the Gaussian transition kernel associated to the Markov chain of the Euler discretization (2.2) of the dynamics (2.1). For each step k ,*

- draw a proposal \tilde{x}_{k+1} according to the kernel $K(x_k, \cdot)$,
- compute the probability

$$p_k = 1 \wedge \frac{K(\tilde{x}_{k+1}, x_k) e^{-\beta_N H_N(\tilde{x}_{k+1})}}{K(x_k, \tilde{x}_{k+1}) e^{-\beta_N H_N(x_k)}}, \quad (2.4)$$

- set $x_{k+1} = \tilde{x}_{k+1}$ with probability p_k ; let $x_{k+1} = x_k$ otherwise.

Note that $K(\cdot, x)$ is Gaussian only if H_N is a quadratic form. Note also that if the proposal kernel K is symmetric in the sense that $K(x, y) = K(y, x)$ for all x, y then it disappears in (2.4), and it turns out that this is the case for the Hybrid Monte Carlo algorithm described next!

A natural issue with these algorithms is the choice of Δt : if it is too large, an important number of steps will be rejected, hence poor convergence properties; conversely, if Δt is too small, many steps will be accepted but the computational cost of evaluating the forces ∇H_N will be prohibitive. This algorithm actually has a nice scaling of the optimal time step Δt with the dimension of the system. Indeed, it can be shown that it scales as $\Delta t \sim N^{-\frac{1}{3}}$, at least for product measures (see [49] and references therein). Although this algorithm is already efficient, we propose to use a kinetic version with further advantages.

2.2. Hybrid Monte Carlo algorithm. Hybrid Monte Carlo is built on Algorithm 2.1, but using a kinetic version of (2.1). For this, a speed variable is introduced so as to improve the exploration of the space. Namely, set $E = \mathbb{R}^{dN}$, and let $U_N : E \rightarrow \mathbb{R}$ be smooth and such that $e^{-\beta_N U_N}$ is Lebesgue integrable. Let $(X_t, Y_t)_{t \geq 0}$ be the diffusion process on $E \times E$ solution to the stochastic differential equation

$$\begin{cases} dX_t &= \alpha_N \nabla U_N(Y_t) dt, \\ dY_t &= -\alpha_N \nabla H_N(X_t) dt - \gamma_N \alpha_N \nabla U_N(Y_t) dt + \sqrt{2 \frac{\gamma_N \alpha_N}{\beta_N}} dB_t, \end{cases} \quad (2.5)$$

where $(B_t)_{t \geq 0}$ is a standard Brownian Motion on E , and $\gamma_N > 0$ is an arbitrary parameter which plays the role of a friction, and which may depend a priori on N even if we do not

use this possibility here. In addition, H_N and β_N are as in (1.1), while U_N plays the role of a generalized kinetic energy [57]. This dynamics admits the following generator:

$$Lf = \underbrace{-\alpha_N \nabla H_N(x) \cdot \nabla_y f + \alpha_N \nabla U_N(y) \cdot \nabla_x f}_{L_1} + \underbrace{\frac{\gamma_N \alpha_N}{\beta_N} \Delta_y f - \gamma_N \alpha_N \nabla U_N(y) \cdot \nabla_y f}_{L_2} \quad (2.6)$$

which leaves invariant the product Boltzmann–Gibbs measure

$$R_N = P_N \otimes Q_N \quad \text{where} \quad Q_N(dy) = \frac{e^{-\beta_N U_N(y)}}{Z'_N} dy,$$

see for instance [56]. In other words

$$R_N(dx, dy) = \frac{e^{-\beta_N \tilde{H}_N(x, y)}}{Z_N Z'_N} dx dy \quad \text{with} \quad \tilde{H}_N(x, y) = H_N(x) + U_N(y). \quad (2.7)$$

As for the overdamped dynamics, the ergodic theorem for additive functionals gives

$$\frac{1}{t} \int_0^t \delta_{(X_s, Y_s)} ds \xrightarrow[t \rightarrow \infty]{\text{weak}} R_N \quad \text{almost surely.}$$

Remark 2.2 (Terms: Hamiltonian, Langevin, overdamped, underdamped, kinetic). *The dynamics (2.5) is called “Hamiltonian” when we turn off the noise by taking $\gamma_N = 0$. On the other hand, when $\gamma_N = \infty$, we recover (2.1) from (2.5). Both (2.1) and (2.5) are known as Langevin dynamics. To be more precise, (2.1) is generally called overdamped while (2.5) is referred to as kinetic or underdamped.*

When $U_N(y) = \frac{1}{2}|y|^2$ then $Y_t = dX_t/dt$, and in this case X_t and Y_t can be interpreted respectively as the *position* and the *velocity* of a system of N points in S at time t . In this case we say that U_N is the *kinetic energy*. For simplicity, we specialize in what follows to this “physical” or “kinetic” case and refer to [57] for more possibilities.

The control of the error or speed of convergence for the HMC algorithm is the subject of active research, see for instance [38] and [7] for some results under structural assumptions.

As before, to simulate $(X_t, Y_t)_{t \geq 0}$, one can discretize (2.5) and sample from a trajectory. This will provide a proposal for the HMC scheme as the Euler discretization (2.2) did for Algorithm 2.1. A good way of doing this is a splitting procedure. First, one integrates the Hamiltonian part *i.e.* the operator L_1 in (2.6), which amounts to a standard Hamiltonian dynamics, before integrating the fluctuation-dissipation part *i.e.* the operator L_2 in (2.6). For discretizing the Hamiltonian dynamics over a time step, a standard approach is the Verlet integrator [41, Sec. 1.2.2], which we describe now. For a time step $\Delta t > 0$, this scheme reads starting from a state (x_k, y_k) at time k :

$$\begin{cases} y_{k+\frac{1}{2}} &= y_k - \nabla H_N(x_k) \alpha_N \frac{\Delta t}{2}, \\ x_{k+1} &= x_k + y_{k+\frac{1}{2}} \alpha_N \Delta t, \\ \tilde{y}_{k+1} &= y_{k+\frac{1}{2}} - \nabla H_N(x_{k+1}) \alpha_N \frac{\Delta t}{2}. \end{cases}$$

This corresponds to updating the velocity over half a time step, then the positions over a time step, and again the velocity over half a time-step. Given that this scheme only corresponds to the Hamiltonian part, it remains to integrate the fluctuation-dissipation part, corresponding to L_2 in (2.6). In this case, it is a simple Ornstein–Uhlenbeck process whose variance can be computed explicitly. Therefore, we add to the previous scheme the

following velocity update which comes from the Mehler formula¹:

$$y_{k+1} = \eta \tilde{y}_{k+1} + \sqrt{\frac{1 - \eta^2}{\beta_N}} G_k, \quad \eta = e^{-\gamma_N \alpha_N \Delta t},$$

where G_k is a standard Gaussian random variable. This integrator leads to averages over an approximation of P_N depending on the time step [39] but, as for the overdamped Langevin dynamics, the singularity of the potential leads to poor approximations. Note that here again, α_N and Δt play the same role.

Hybrid or Hamiltonian Monte Carlo (HMC) methods, built on the later integration, appeared in theoretical physics in lattice quantum chromodynamics with [17], and are still actively studied in applied mathematics, see for instance [4, 57, 41, 8] and references therein. The HMC algorithm can be thought of in a sense as a special Metropolis Adjusted (underdamped) Langevin Algorithm. Indeed, inspired by the MALA Algorithm 2.1, a way to avoid the stability problem of the discretization of the kinetic Langevin dynamics mentioned above is to add an acceptance-rejection step. A surprising advantage of this approach is that the Verlet integration scheme is time reversible up to momenta reversal [41, Sec. 2.1.3 and eq. (2.11)], hence when computing the acceptance probability as in (2.4), the transition kernel does not appear. Let us now describe the algorithm.

Algorithm 2.3 (HMC). *Start from a configuration (x_0, y_0) and perform the following steps for each time $k \geq 0$:*

- (1) *update the velocities with*

$$\tilde{y}_k = \eta y_k + \sqrt{\frac{1 - \eta^2}{\beta_N}} G_k, \quad \eta = e^{-\gamma_N \alpha_N \Delta t};$$

- (2) *run one step of the Verlet scheme:*

$$\begin{cases} y_{k+\frac{1}{2}} &= \tilde{y}_k - \nabla H_N(x_k) \alpha_N \frac{\Delta t}{2} \\ \tilde{x}_{k+1} &= x_k + y_{k+\frac{1}{2}} \alpha_N \Delta t \\ \tilde{y}_{k+1} &= y_{k+\frac{1}{2}} - \nabla H_N(x_{k+1}) \alpha_N \frac{\Delta t}{2}; \end{cases} \quad (2.8)$$

- (3) *compute the probability ratio*

$$p_k = 1 \wedge \exp\left[-\beta_N \left(H_N(\tilde{x}_{k+1}) + \frac{\tilde{y}_{k+1}^2}{2} - H_N(x_k) - \frac{y_k^2}{2}\right)\right];$$

- (4) *set*

$$(x_{k+1}, y_{k+1}) = \begin{cases} (\tilde{x}_{k+1}, \tilde{y}_{k+1}) & \text{with probability } p_k, \\ (x_k, -y_k) & \text{with probability } 1 - p_k. \end{cases}$$

As noted in the various references above, the Metropolis step acts as a corrector on the energy conservation of the Hamiltonian step. In this, it helps avoiding irrelevant moves, while enhancing the exploration capacities of the dynamics through the speed variable. A more precise argument in favor of this algorithm is the scaling of the time step Δt with respect to the system size N . Indeed, as shown in [4] for product measures, the optimal scaling is as $\Delta t \sim N^{-\frac{1}{4}}$, which makes the algorithm appealing for large systems. Since the Hamiltonian computational cost scales as N^2 , we see that the cost of the algorithm for a fix time T and $N = \lceil T/\Delta t \rceil$ is in $\mathcal{O}(N^{\frac{9}{4}})$, which has to be compared to the $\mathcal{O}(N^4)$ reached in [44]. Finally, the parameter γ_N can also be tuned in order to optimize the speed of convergence – we leave this detail here and stick to $\gamma_N = 1$.

¹The Mehler formula states that the Ornstein–Uhlenbeck process $(Z_t)_{t \geq 0}$ in \mathbb{R}^n solution of the stochastic differential equation $dZ_t = \sqrt{2\sigma^2} dB_t - \rho Z_t dt$ satisfies $\text{Law}(Z_{t+s} | Z_s = z) = \mathcal{N}(ze^{-\rho t}, \frac{1 - e^{-2\rho t}}{\rho} \sigma^2 I_n)$.

From a practical point of view, the algorithm can be tested in the following way. First, when only the Hamiltonian part of the dynamics is integrated with the Verlet scheme, it can be checked that the energy error scales as Δt^3 as $\Delta t \rightarrow 0$. Then, if the selection step is added, the rejection rate should also scale as Δt^3 . When the speed resampling is added, this rejection rate scaling should not change. This has been checked for the implementation proposed in appendix – we do not reproduce the plots for brevity. In practice, we choose Δt on a simple empirical basis in order to have a small rejection rate, which could be optimized.

3. NUMERICAL EXPERIMENTS ON REMARKABLE MODELS

In this section, we start testing Algorithm 2.3 for the two cases described in Section 1.4. Since the equilibrium measures are known for any $N \geq 2$, we will be able to compare accurately our results with the expected one. We will also consider models for which the empirical spectral distribution and the equilibrium distribution are not known. We remind that when $S = \mathbb{R}^d$ with $d \geq 1$ we have the following formulas that hold in any dimension:

$$\nabla |x|^2 = 2x, \quad \nabla \log \frac{1}{|x|} = -\frac{x}{|x|^2}, \quad \nabla \frac{1}{|x|} = -\frac{x}{|x|^3}.$$

3.1. Case study: 1D. We test the numerical method by looking at the mean empirical distribution in the case of the Gaussian Unitary Ensemble (1.2) with $\beta = 2$, $N = 8$, for which the exact expression of $\mathbb{E}\mu_N$ under P_N is provided by (1.3). The results in Figure 2 show a very good agreement between the exact result and the algorithm.

For completeness, we also study the quartic confinement potential $V(x) = x^4/4$, as in [44]. In this case, the empirical spectral distribution is not known, but the equilibrium distribution has density with respect to the Lebesgue measure given by

$$x \in \mathbb{R} \mapsto (2a^2 + x^2) \frac{\sqrt{4a^2 - x^2}}{2\pi} \mathbf{1}_{x \in [-2a, 2a]}, \quad a = 3^{-\frac{1}{4}}.$$

The results of the numerical simulations, see Figure 3, show a good agreement with the equilibrium measure when N is large. Note that for such a Coulomb gas with quartic confinement, to our knowledge, no matrix model with independent entries is known.

3.2. Case study: 2D. We next consider in Figure 4 the mean empirical distribution in the case of the Complex Ginibre Ensemble (1.5) with $\beta = 2$, $N = 8$. In this case, we also know a theoretical formula for $\mathbb{E}\mu_N$ under P_N , given by (1.6). One could also check the Gumbel fluctuation at the edge, which is proved for $\beta = 2$ and conjectured for $\beta \neq 2$, see [12, 18] (note that in this case we have a formula for μ_* but not for $\mathbb{E}\mu_N$ under P_N). One could also explore the crystallization phenomenon, see [5] and references therein.

3.3. Case study: 3D. In Figure 5, we finally turn to the Coulomb gas which corresponds to $S = \mathbb{R}^3$, $d = n = 3$, $V = |\cdot|^2/\beta$, $W = 1/|\cdot|$ and to the log-gas for which $W = -\log |\cdot|$. In the first case the equilibrium measure μ_* is uniform on the centered ball of \mathbb{R}^d of radius $((\beta(d-2)/2)^{1/d})$, see for instance [11, Cor. 1.3], while in the second case the equilibrium measure is not known yet, see however [13]. In both cases we do not have a formula for $\mathbb{E}\mu_N$ under P_N . One could study the fluctuation at the edge, which is conjectured to be Gumbel, just like for the complex Ginibre ensemble in 2D.

APPENDIX A. JULIA CODE

Here is a program written in the Julia language² illustrating our method. It allows to exploit the multiple cores of modern processors and works in parallel on clusters. Beware

²<http://JuliaLang.org/>

that this code is not fully optimized, for instance the energy and its gradient could be computed simultaneously for better performance.

```

1 #-----#
2 #----- Simulating coulomb gases with HMC algorithm -----#
3 #-----#
4
5 @everywhere begin # for parallel computing with julia -p NumberOfAdditionalCPU
6
7 #-----#
8 # Customization part : parameters, confinement, and interaction #
9 #-----#
10
11 ## Parameters. Note that in this code  $U_N(y)=|y|^2/2$ .
12
13 # Final time and time step
14 const T = 1e4
15 const dt = 0.1
16 # Number of eigenvalues
17 const N = 50
18 # Dimension of the physical space
19 const dim = 1 # works for dimensions 1, 2, 3
20 # Temperature and friction
21 const beta = 2.
22
23 ## Functions
24
25 # Confinement potential V and its gradient
26 @inline function confinement(x)
27     return dot(x,x)/(2*beta) # 1D Beta-Hermite
28     # return dot(x,x)/beta # 2D Beta-Ginibre, 3D Beta-Coulomb
29 end
30 @inline function confinement_gradient(x)
31     return x/beta # 1D Beta-Hermite
32     # return 2*x/beta # 2D Beta-Ginibre, 3D Beta-Coulomb
33 end
34
35 # Interaction potential W and its gradient
36 @inline function interaction(x,y)
37     return -log(norm(x-y)) # 1D Beta-H., 2D Beta-Gin., 2D/3D Beta log-gas.
38     # return 1/norm(x-y) # 3D Beta-Coulomb
39 end
40 @inline function interaction_gradient(x,y)
41     v = x-y
42     return -v/norm(v)^2 # 1D Beta-H., 2D Beta-Gin
43     # return -v/norm(v)^3 # 3D Beta-Coulomb
44 end
45
46 #-----#
47 #----- Parameters computed from inputs -----#
48 #-----#
49
50 const alphan = 1.
51 const betan = beta * N^2
52 const gamman = 1. / alphan
53 # Parameters for discretisation of fluctuation-dissipation part L2
54 const etan = exp(- gamman * alphan * dt)
55 const sdn = sqrt((1-etan^2)/betan)
56 #-- I/O parameter, write the configuration every "freq" steps
57 const freq = 1000
58 # Number of iterations and number of outputs
59 const niter = Int64(round(T/dt))
60 const nsteps = Int64(round(niter/freq))
61
62 #-----#
63 #----- Core part - Be careful and good luck! -----#
64 #-----#
65
66 ## Functions
67
68 # Potential energy  $H_N$ 
69 @inline function energy(X)
70     ener = 0
71     @inbounds for i = 1:N
72         @inbounds for j = i+1:N
73             ener += interaction(X[i],X[j]) /N
74         end
75     end
76     ener += confinement(X[i])
77     return ener /N
78 end # function energy()
79
80 # Kinetic energy  $U_N$ 

```

```

81     @inline function kinetic(Y)
82         return norm(Y)^2 / 2.
83     end # function kinetic()
84
85     # Force applied on particle at X[i] from all others at positions X[j] j!=i
86     @inline function compute_force!(X,F) # -Grad H_N
87         # Computation of interaction forces between each pairs
88         Fpairs = Array{Vector{Float64}}(N,N) # we use only N(N-1)/2 entries
89         @inbounds for i = 1:N
90             @inbounds for j = 1:i-1
91                 Fpairs[i,j] = -interaction_gradient(X[i],X[j])
92             end
93         end
94         # Computation of total force on each particle
95         @inbounds for i = 1:N
96             F[i] = zeros(dim)
97             # Interaction
98             @inbounds for j = 1:i-1
99                 F[i] += Fpairs[i,j]
100            end
101            @inbounds for j = i+1:N
102                F[i] -= Fpairs[j,i]
103            end
104            F[i] /= N
105            # Confinement
106            F[i] -= confinement_gradient(X[i])
107            F[i] /= N
108        end
109    end # function compute_force!()
110
111    # compute the new force and speed
112    @inline function verlet_integrator!(Fnew, Fcur, Xnew, Ynew, X, Y)
113        @inbounds for i=1:N
114            Ynew[i] = Y[i] + Fcur[i] * alphan * dt/2.
115            Xnew[i] = X[i] + Ynew[i] * alphan * dt
116        end
117        compute_force!(Xnew,Fnew)
118        @inbounds for i=1:N
119            Ynew[i] += Fnew[i] * alphan * dt/2
120        end
121    end # function verlet_integrator!()
122
123    # update positions and speed
124    function update!(X, Y, Fcur, Xnew, Ynew, Fnew, Epot, acceptrate)
125        #--- Speed resampling
126        @inbounds for i = 1:N
127            Y[i] = etan * Y[i] + sdn * randn(dim)
128        end
129        Ekin = kinetic(Y)
130        Energy = Epot + Ekin
131        #--- Verlet integrator. Position-speed proposal will be in (Xnew,Ynew).
132        verlet_integrator!(Fnew, Fcur, Xnew, Ynew, X, Y)
133        # New energy
134        Epotnew = energy(Xnew)
135        Ekinnew = kinetic(Ynew)
136        NewEnergy = Epotnew + Ekinnew
137        # Metropolis ratio
138        r = beta * (- NewEnergy + Energy)
139        # Selection-rejection step
140        if log(rand()) <= r
141            # acceptance
142            @inbounds @simd for i = 1:N
143                X[i] = Xnew[i]
144                Y[i] = Ynew[i]
145                Fcur[i] = Fnew[i]
146            end
147            acceptrate[1] += 1
148            Epot = Epotnew
149        else # rejection: speed inversion
150            @inbounds @simd for i = 1:N
151                Y[i] = -Y[i]
152            end
153        end
154        return Epot
155    end # function update()
156
157    # Runs a trajectory of HMC algorithm and compute averages
158    function HMC(runid_is_useless)
159        #--- For output : table where the position are written every freq steps
160        Trajectory = Array{Float64}(nsteps,N*dim)
161        #--- For output : Acceptation rate for the HMC selection step
162        acceptrate = zeros(1)
163        # Local variables
164        #--- configuration and speed

```

```

165 X = Vector{Vector{Float64}}(N)
166 Y = Vector{Vector{Float64}}(N)
167 #--- initial forces
168 Fcur = Vector{Vector{Float64}}(N)
169 #--- Same quantities for the proposal
170 Ynew = Vector{Vector{Float64}}(N)
171 Xnew = Vector{Vector{Float64}}(N)
172 Fnew = Vector{Vector{Float64}}(N)
173 #--- norms for the statistics of the max
174 Norms = zeros(niter)
175 # random initial configuration with uniform law on a square
176 for i = 1:N
177     X[i] = -1 + 2 * rand(dim)
178 end
179 # Initial zero speed and forces
180 for i = 1:N
181     Y[i] = zeros(dim)
182     Fcur[i] = zeros(dim)
183     Xnew[i] = X[i]
184     Ynew[i] = Y[i]
185     Fnew[i] = Fcur[i]
186 end
187 #--- initialization of different quantities
188 Ekin = kinetic(Y)
189 Epot = energy(X)
190 Energy = Epot + Ekin
191 #--- Loop over time
192 @fastmath @inbounds for n = 1:niter
193     #--- save configuration every freq steps
194     if n % freq == 0
195         for i = 1:N
196             for k = 1:dim
197                 Trajectory[ Int64(n/freq), (i-1) * dim + k ] = X[i][k]
198             end
199         end
200     end
201     #--- update positions and speeds
202     Epot = update!( X, Y, Fcur, Xnew, Ynew, Fnew, Epot, acceptrate)
203
204 end
205 return (acceptrate, Trajectory)
206 end # function HMC()
207 #
208 end # @everywhere
209
210 ### Main part - runs only on main instance of Julia.
211
212 Nprocs = nprocs()
213 print("Number of processors ", Nprocs, ".\n")
214 print("Time of the simulation ", T, ".\n")
215 print("Number of time steps ", T/dt, ".\n")
216
217 ## Launching computations on Nprocs parallel processors
218 output = @time pmap(HMC, 1:Nprocs)
219
220 ## Post-processing
221 for run in 1:Nprocs
222     acceptrate = output[run][1]
223     Trajectory = output[run][2]
224     print("Percentage of rejected steps: ", 1-acceptrate/niter, "\n")
225     ## Post processing
226     # some reordering for histogram plot
227     Positions=Array{Float64}(N*nsteps, dim)
228     for n = 1:nsteps
229         for i = 1:N
230             for k = 1:dim
231                 Positions[ (n-1)*N + i, k ] = Trajectory[n, (i-1)*dim + k]
232             end
233         end
234     end
235     # computation of the radius, and the maximal radius
236     Radii = Array{Float64}(N*nsteps)
237     Maxima = Array{Float64}(nsteps)
238     for n = 1:nsteps
239         maxRadius = 0
240         for i = 1:N
241             radius = norm( Positions[ (n-1)*N + i, : ] )
242             Radii[ (n-1)*N + i ] = radius
243             if radius > maxRadius
244                 maxRadius = radius
245             end
246         end
247         Maxima[n] = maxRadius
248     end

```

```

249 # Write the data in text files – Whole trajectory sample
250 writedlm(@sprintf("output-%i",run), Positions, " ")
251 writedlm(@sprintf("maxoutput-%i",run), Maxima, " ")
252 writedlm(@sprintf("distoutput-%i",run), Radii, " ")
253 end # for run

```

Acknowledgments. We warmly thank Gabriel Stoltz for his encouragements and for very useful discussions on the theoretical and numerical sides of this work.

REFERENCES

- [1] G. W. ANDERSON, A. GUIONNET & O. ZEITOUNI – *An Introduction to Random Matrices*, Cambridge Studies in Advanced Mathematics, vol. 118, Cambridge University Press, Cambridge, 2010. 6
- [2] R. BARDENET & A. HARDY – “Monte Carlo with Determinantal Point Processes”, preprint arXiv:1605.00361v1, 2016. 5
- [3] R. J. BERMAN – “On large deviations for Gibbs measures, mean energy and Gamma-convergence”, preprint arXiv:1610.08219v1, 2016. 3
- [4] A. BESKOS, N. PILLAI, G. ROBERTS, J.-M. SANZ-SERNA & A. STUART – “Optimal tuning of the hybrid Monte Carlo algorithm”, *Bernoulli* **19** (2013), no. 5A, p. 1501–1534. 1, 9
- [5] X. BLANC & M. LEWIN – “The crystallization conjecture: a review”, *EMS Surv. Math. Sci.* **2** (2015), no. 2, p. 225–306. 10
- [6] F. BOLLEY, D. CHAFAÏ & J. FONTBONA – “Dynamics of a planar Coulomb gas”, preprint arXiv:1706.08776v3 to appear in *Annals of Applied Probability*, 2017. 6
- [7] N. BOU-RABEE, A. EBERLE & R. ZIMMER – “Coupling and Convergence for Hamiltonian Monte Carlo”, preprint arXiv:1805.00452v1, 2018. 8
- [8] N. BOU-RABEE & J. M. SANZ-SERNA – “Geometric integrators and the Hamiltonian Monte Carlo method”, preprint arXiv:1711.05337, 2017. 1, 9
- [9] S. BROOKS, A. GELMAN, G. L. JONES & X.-L. MENG (eds.) – *Handbook of Markov Chain Monte Carlo*, Chapman & Hall/CRC Handbooks of Modern Statistical Methods, CRC Press, Boca Raton, FL, 2011. 5
- [10] N. BROSSE, A. DURMUS, É. MOULINES & S. SABANIS – “The tamed unadjusted Langevin algorithm”, preprint arXiv:1710.05559v2, 2017. 6
- [11] D. CHAFAÏ, N. GOZLAN & P.-A. ZITT – “First-order global asymptotics for confined particles with singular pair repulsion”, *Ann. Appl. Probab.* **24** (2014), no. 6, p. 2371–2413. 3, 10
- [12] D. CHAFAÏ & S. PÉCHÉ – “A note on the second order universality at the edge of Coulomb gases on the plane”, *J. Stat. Phys.* **156** (2014), no. 2, p. 368–383. 10
- [13] D. CHAFAÏ & E. SAFF – “Aspects of an Euclidean log-gas”, work in progress, 2018. 3, 10
- [14] D. CHAFAÏ, A. HARDY & M. MAÏDA – “Concentration for Coulomb gases and Coulomb transport inequalities”, preprint arXiv:1610.00980v3 to appear in *J. Funct. Anal.*, 2018. 3
- [15] D. CHAFAÏ & J. LEHEC – “On Poincaré and logarithmic Sobolev inequalities for a class of singular Gibbs measures”, preprint arXiv:1805.00708v2, 2018. 6
- [16] L. DECREUSEFOND, I. FLINT & A. VERGNE – “A note on the simulation of the Ginibre point process”, *J. Appl. Probab.* **52** (2015), no. 4, p. 1003–1012. 5
- [17] S. DUANE, A. KENNEDY, B. J. PENDLETON & D. ROWETH – “Hybrid Monte Carlo”, *Physics Letters B* **195** (1987), no. 2, p. 216–222. 9
- [18] G. DUBACH – “Powers of Ginibre Eigenvalues”, arXiv:1711.03151v2, 2017. 10
- [19] I. DUMITRIU & A. EDELMAN – “Matrix models for beta ensembles”, *J. Math. Phys.* **43** (2002), no. 11, p. 5830–5847. 4
- [20] A. B. DUNCAN, T. LELIÈVRE & G. A. PAVLIOTIS – “Variance Reduction Using Nonreversible Langevin Samplers”, *J. Stat. Phys.* **163** (2016), p. 457–491. 6
- [21] A. B. DUNCAN, N. NÜSKEN & G. A. PAVLIOTIS – “Using perturbed underdamped Langevin dynamics to efficiently sample from probability distributions”, *J. Stat. Phys.* **169** (2017), no. 6, p. 1098–1131. 5
- [22] A. EDELMAN & N. R. RAO – “Random matrix theory”, *Acta Numer.* **14** (2005), p. 233–297. 4
- [23] L. ERDŐS & H.-T. YAU – *A dynamical approach to random matrix theory*, Courant Lecture Notes in Mathematics, vol. 28, Courant Institute of Mathematical Sciences, New York; American Mathematical Society, Providence, RI, 2017. 6
- [24] Z. F. EZAWA – *Quantum Hall effects*, second ed., World Scientific Publishing Co. Pte. Ltd., Hackensack, NJ, 2008, Field theoretical approach and related topics. 5
- [25] P. J. FORRESTER – *Log-gases and Random Matrices*, London Mathematical Society Monographs Series, vol. 34, Princeton University Press, Princeton, NJ, 2010. 4, 5
- [26] P. J. FORRESTER – “Analogies between random matrix ensembles and the one-component plasma in two-dimensions”, *Nuclear Phys. B* **904** (2016), p. 253–281. 4

- [27] D. GARCÍA-ZELADA – “A large deviation principle for empirical measures on Polish spaces: Application to singular Gibbs measures on manifolds”, preprint arXiv:1703.02680v2, 2017. 3
- [28] A. HARDY – “Polynomial Ensembles and Recurrence Coefficients”, arXiv:1709.01287v1, 2017. 5
- [29] L. L. HELMS – *Potential Theory*, second ed., Universitext, Springer, London, 2014. 3
- [30] T. A. HÖFT & B. K. ALPERT – “Fast updating multipole Coulombic potential calculation”, *SIAM J. Sci. Comput.* **39** (2017), no. 3, p. A1038–A1061. 6
- [31] J. B. HOUGH, M. KRISHNAPUR, Y. PERES & B. VIRÁG – “Determinantal processes and independence”, *Probab. Surv.* **3** (2006), p. 206–229. 5
- [32] M. HUTZENTHALER, A. JENTZEN & P. E. KLOEDEN – “Strong convergence of an explicit numerical method for SDEs with nonglobally lipschitz continuous coefficients”, *Ann. Appl. Probab.* **22** (2012), no. 4, p. 1611–1641. 6
- [33] T. JIANG & Y. QI – “Spectral radii of large non-Hermitian random matrices”, *J. Theoret. Probab.* **30** (2017), no. 1, p. 326–364. 4
- [34] P. E. KLOEDEN, E. PLATEN & H. SCHURZ – *Numerical solution of SDE through computer experiments*, Universitext, Springer-Verlag, Berlin, 1994, With 1 IBM-PC floppy disk (3.5 inch; HD). 7
- [35] N. S. LANDKOF – *Foundations of Modern Potential Theory*, Springer-Verlag, New York-Heidelberg, 1972, Translated from the Russian by A. P. Doohovskoy, Die Grundlehren der mathematischen Wissenschaften, Band 180. 3
- [36] F. LAVANCIER, J. MØLLER & E. RUBAK – “Determinantal point process models and statistical inference”, *J. R. Stat. Soc. Ser. B. Stat. Methodol.* **77** (2015), no. 4, p. 853–877. 5
- [37] M. LEDOUX – “Differential operators and spectral distributions of invariant ensembles from the classical orthogonal polynomials. The continuous case”, *Electron. J. Probab.* **9** (2004), p. no. 7, 177–208. 4
- [38] Y. T. LEE & S. S. VEMPALA – “Convergence Rate of Riemannian Hamiltonian Monte Carlo and Faster Polytope Volume Computation”, preprint arXiv:1710.06261v1, 2017. 8
- [39] B. LEIMKUHNER, C. MATTHEWS & G. STOLTZ – “The computation of averages from equilibrium and nonequilibrium Langevin molecular dynamics”, *IMA J. Numer. Anal.* **36** (2015), no. 1, p. 13–79. 9
- [40] T. LELIÈVRE, F. NIER & G. A. PAVLIOTIS – “Optimal Non-reversible Linear Drift for the Convergence to Equilibrium of a Diffusion”, *J. Stat. Phys.* **152** (2013), p. 237–274. 6
- [41] T. LELIÈVRE, M. ROUSSET & G. STOLTZ – *Free Energy Computations. A Mathematical Perspective*, Imperial College Press, London, 2010. 8, 9
- [42] ———, “Langevin dynamics with constraints and computation of free energy differences”, *Math. Comp.* **81** (2012), no. 280, p. 2071–2125. 2
- [43] T. LELIÈVRE & G. STOLTZ – “Partial differential equations and stochastic methods in molecular dynamics”, *Acta Numer.* **25** (2016), p. 681–880. 5
- [44] X. H. LI & G. MENON – “Numerical solution of Dyson Brownian motion and a sampling scheme for invariant matrix ensembles”, *J. Stat. Phys.* **153** (2013), no. 5, p. 801–812. 1, 6, 7, 9, 10
- [45] M. L. MEHTA – *Random Matrices*, third ed., Pure and Applied Mathematics (Amsterdam), vol. 142, Elsevier/Academic Press, Amsterdam, 2004. 4, 5
- [46] G. N. MILSTEIN & M. V. TRETYAKOV – *Stochastic Numerics for Mathematical Physics*, Springer Science & Business Media, 2013. 7
- [47] S. OLVER, R. R. NADAKUDITI & T. TROGDON – “Sampling unitary ensembles”, *Random Matrices Theory Appl.* **4** (2015), no. 1, p. 1550002, 22. 5
- [48] C. P. ROBERT & G. CASELLA – *Monte Carlo Statistical Methods*, second ed., Springer Texts in Statistics, Springer-Verlag, New York, 2004. 7
- [49] G. O. ROBERTS & J. S. ROSENTHAL – “Optimal scaling for various Metropolis-Hastings algorithms”, *Statistical science* **16** (2001), no. 4, p. 351–367. 7
- [50] E. B. SAFF & V. TOTIK – *Logarithmic Potentials with External Fields*, Grundlehren der Mathematischen Wissenschaften [Fundamental Principles of Mathematical Sciences], vol. 316, Springer-Verlag, Berlin, 1997, Appendix B by Thomas Bloom. 3
- [51] A. SCARDICCHIO, C. E. ZACHARY & S. TORQUATO – “Statistical properties of determinantal point processes in high-dimensional Euclidean spaces”, *Phys. Rev. E (3)* **79** (2009), no. 4, p. 041108, 19. 5
- [52] S. SERFATY – *Coulomb gases and Ginzburg-Landau vortices*, Zurich Lectures in Advanced Mathematics, Euro. Math. Soc. (EMS), Zürich, 2015. 3, 4
- [53] ———, “Systems of points with Coulomb interactions”, preprint arXiv:1712.04095v1, 2017. 3, 4
- [54] S. SMALE – “Mathematical problems for the next century”, *Math. Intelligencer* **20** (1998), no. 2, p. 7–15. 3
- [55] ———, “Mathematical problems for the next century”, in *Mathematics: frontiers and perspectives*, Amer. Math. Soc., Providence, RI, 2000, p. 271–294. 3
- [56] G. STOLTZ & Z. TRSTANOVA – “Langevin dynamics with general kinetic energies”, preprint arXiv:1609.02891v5, 2016. 8

- [57] ———, “Stable and accurate schemes for Langevin dynamics with general kinetic energies”, preprint arXiv:1609.02891v1, 2016. 6, 8, 9

(DC) UNIVERSITÉ PARIS-DAUPHINE, PSL, CNRS, CEREMADE, F-75016 PARIS, FRANCE

E-mail address: [mailto:djalil\(at\)chafai.net](mailto:djalil(at)chafai.net)

URL: <http://djalil.chafai.net/>

(GF) UNIVERSITÉ PARIS-EST, CERMICS (ENPC), INRIA, F-77455 MARNE-LA-VALLÉE, FRANCE

E-mail address: <mailto:gregoire.ferre@enpc.fr>

URL: <https://team.inria.fr/materials/team-members/gregoire-ferre/>

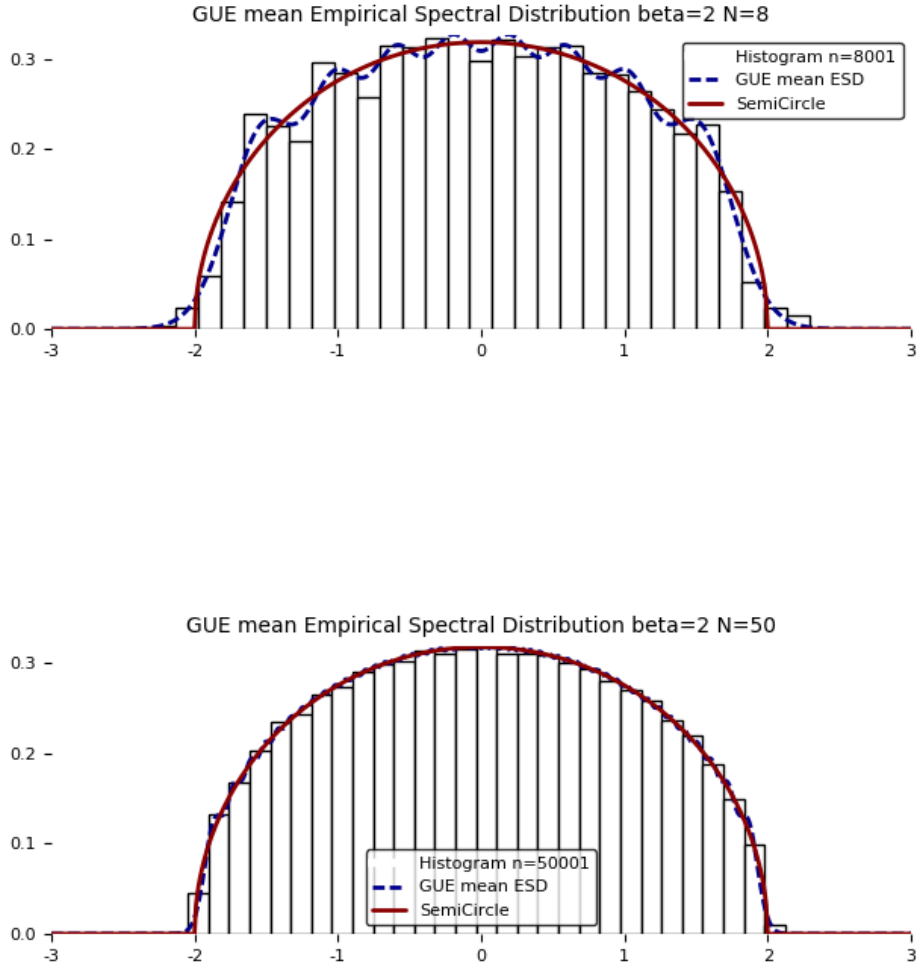


FIGURE 2. Study of the Gaussian Unitary Ensemble with $N = 8$ (top) and $N = 50$ (bottom). The solid line is the plot of the limiting spectral distribution (1.4) while the dashed line is the plot of the mean empirical distribution (1.3). The bars form the histogram of simulations obtained using our HMC algorithm. This algorithm was run 1 times with final-time $T = 10^6$ and time-step $\Delta t = 0.5$. The histogram was produced by looking at the last half of the trajectory and retaining the positions each 1000 time-steps, producing n values, namely $\approx 8 \times 10^3$ and $\approx 5 \times 10^4$ respectively.

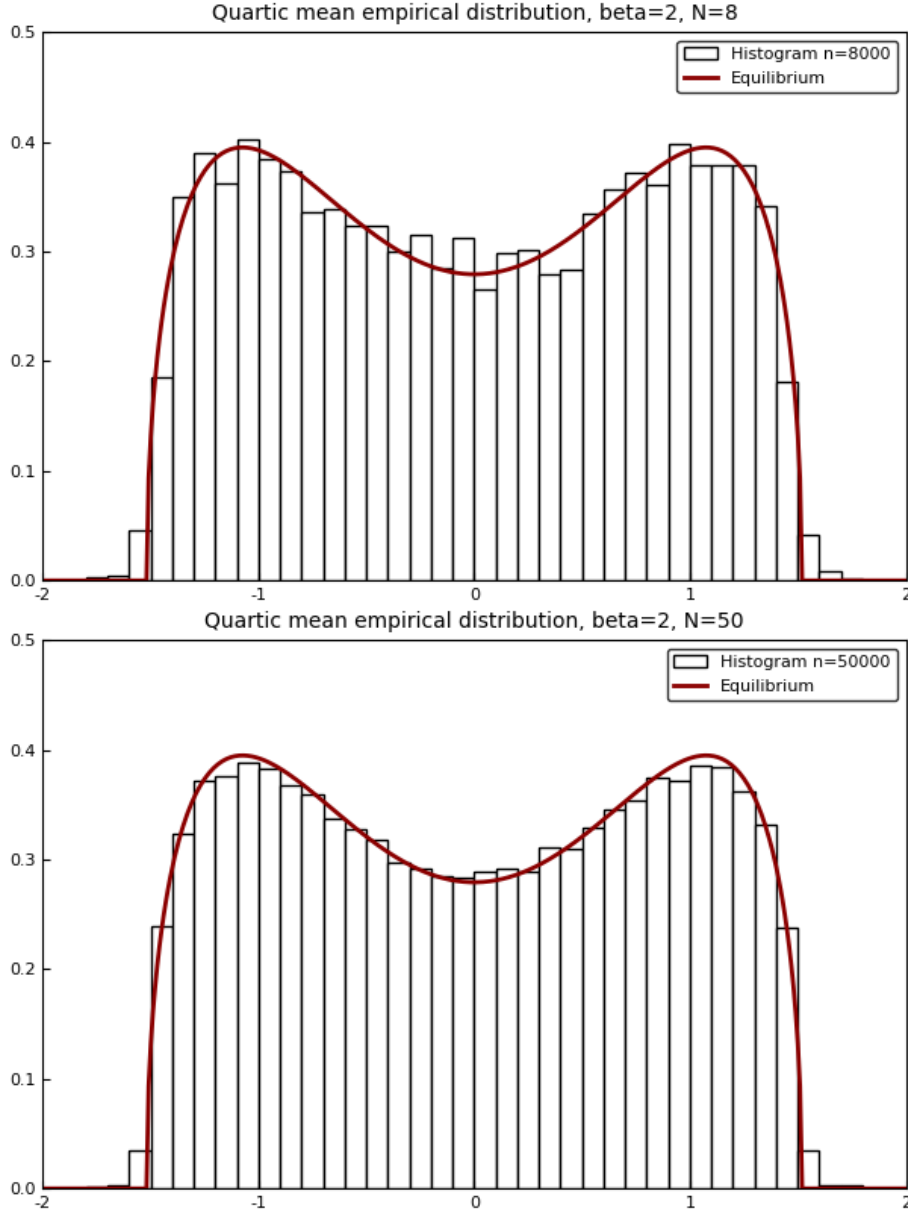


FIGURE 3. Study of the quartic confinement with $N = 8$ (top) and $N = 50$ (bottom). The solid line is the plot of the limiting spectral distribution (1.4). The bars form the histogram of simulations obtained using our HMC algorithm. This algorithm was run once with final-time $T = 10^6$ and time-step $\Delta t = 0.5$. The histogram was produced by looking at the last half of the trajectory and retaining the positions each 1000 time-steps, producing n values namely $\approx 8 \times 10^3$ and $\approx 5 \times 10^4$ respectively. We do not have a formula for the mean empirical distribution for this model.

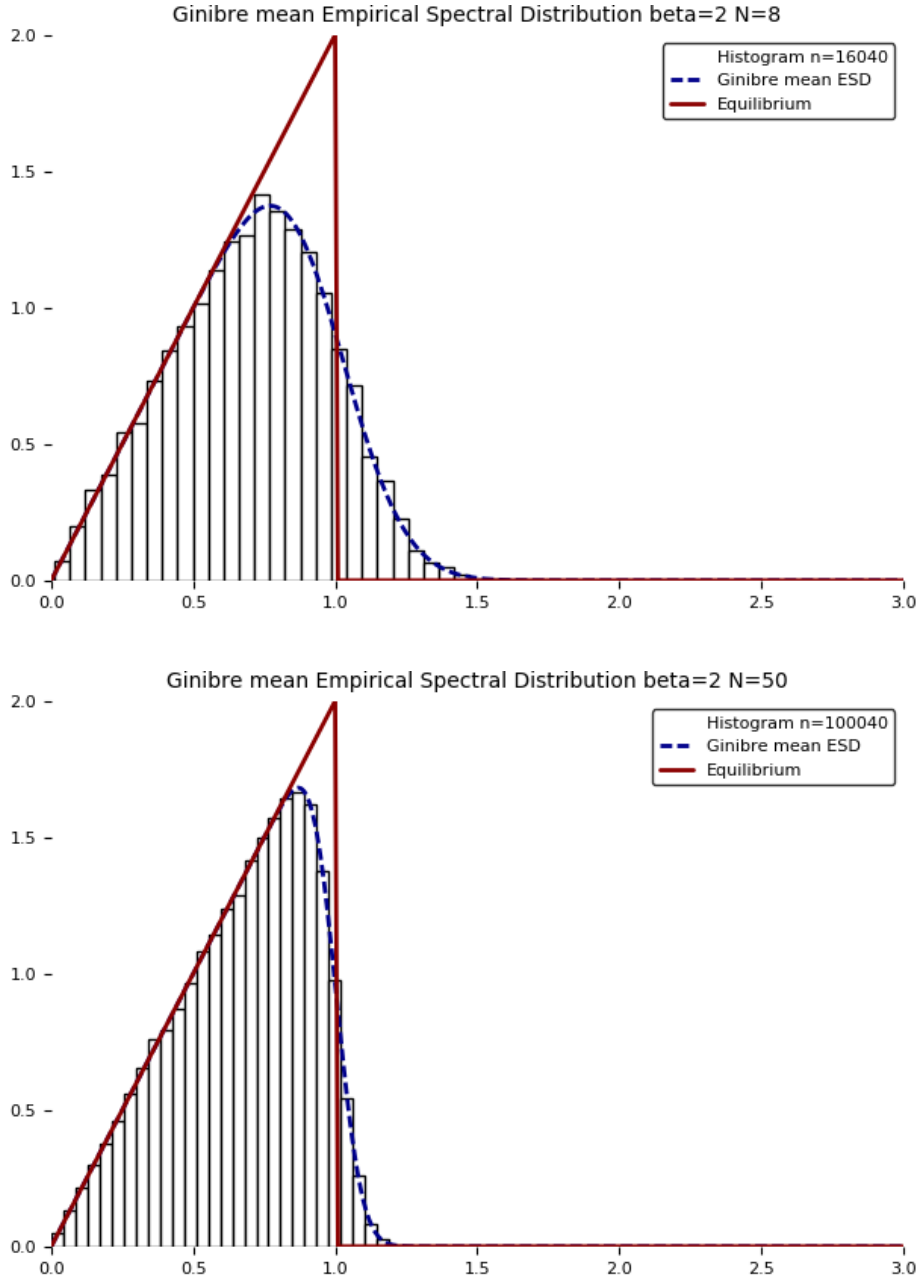


FIGURE 4. Study of the complex Ginibre ensemble with $N = 8$ (top) and $N = 50$ (bottom). The solid line is the plot of the limiting spectral distribution (1.7) while the dashed line is the plot of the mean empirical distribution (1.6), both as functions of the radius $|z|$ and scaled by 2π (in order to obtain a radial density). The bars form the histogram of simulations obtained using our HMC algorithm. This algorithm was run 40 times with final-time $T = 10^5$ and time-step $\Delta t = 0.1$. The histogram was produced by looking at the last halves of the 40 trajectories and retaining the positions each 10000 time-steps, producing n values namely $\approx 16 \times 10^3$ and $\approx 10^5$ respectively.

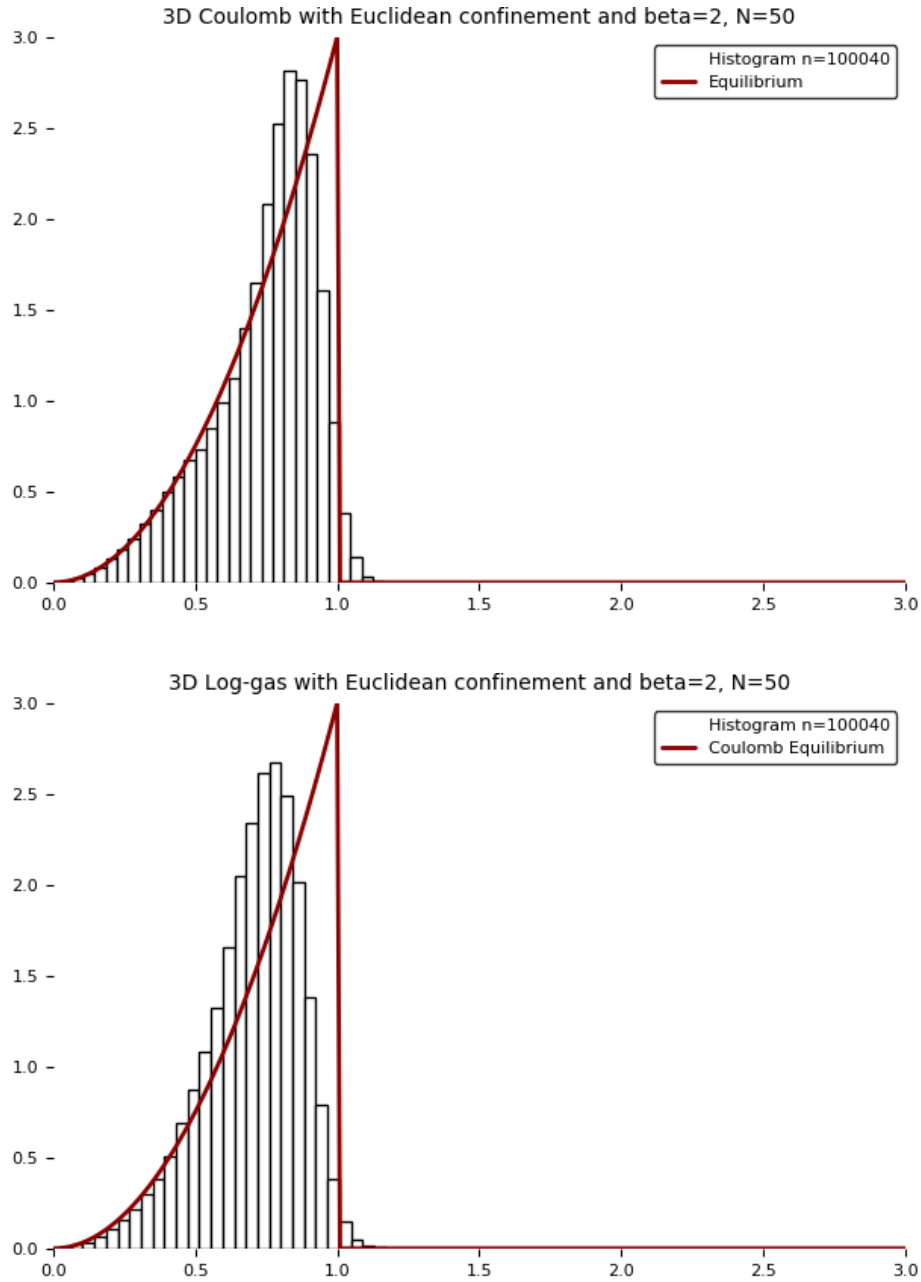


FIGURE 5. Study of the 3D Coulomb case (top) and 3D Log-gas (bottom) with Euclidean confinement and $\beta = 2$ and $N = 50$. Equilibrium measure in solid line and histogram obtained with our HMC algorithm with $N = 50$ and same simulation parameters as for Figure 4. In contrast with the GUE case and the Ginibre case, we do not have a formula for the mean empirical distribution at fixed N for both cases, and for the Log-gas (bottom) the equilibrium measure is not known.